ISSN 1066-3622, Radiochemistry, 2026, Vol. 68, No. 5, pp. 583–593. © Pleiades Publishing, Inc., 2026.

"2 + 1" Tricarbonyl Complexes of Technetium-99 and Rhenium with NN-Aromatic Diimines and 1-Adamantyl Isocyanide: Synthesis and Structure

A. E. Miroslavov[a,b,c,*], E. S. Babitova[a,b,c], M. Yu. Tyupina[a,b,c], A. A. Brechalov[a,b,c], V. V. Gurzhiy[d], A. P. Sakhonenkova[a,c], E. V. Kozlova[b], L. S. Chisty[e], and M. A. Kinzhalov[f]

[a] *Khlopin Radium Institute, St. Petersburg, 194021 Russia*
[b] *Chair of Radiochemistry, St. Petersburg State University, St. Petersburg, 199034 Russia*
[c] *Ozyorsk Institute of Technology, National Research Nuclear University MEPhI, Ozyorsk, Chelyabinsk oblast, 456783 Russia*
[d] *Chair of Crystal Chemistry, St. Petersburg State University, St. Petersburg, 199034 Russia*
[e] *Research Institute of Hygiene, Professional Pathology, and Ecology of Human, Kuzmolovskii, Vsevolozhsk raion, Leningrad oblast, 188663 Russia*
[f] *Chair of Physical Organic Chemistry, St. Petersburg State University, St. Petersburg, 199034 Russia*
**e-mail: amiroslav@mail.ru*

Received September 9, 2026; revised October 2, 2026; accepted October 9, 2026

Abstract—"2 + 1" tricarbonyl complexes of technetium(I) and rhenium(I) $[M(NN)(CO)_3(CNAd)]ClO_4$ (M = ^{99}Tc, Re; NN = 2,2'-bipyridine (bipy) or 1,10-phenanthroline (phen); CNAd = 1-adamantyl isocyanide) were prepared by the reaction of $[M(ClO_4)(CO)_5]$ with the corresponding diimine in ethanol, followed by replacement of the coordinated solvent molecule in the intermediate $[M(NN)(CO)_3(EtOH,H_2O)]ClO_4$ by CNAd. The compounds were characterized in solution by IR and ^{1}H, ^{99}Tc NMR spectroscopy. The molecular structure of the crystalline complexes $[^{99}Tc(bipy)(CO)_3(CNAd)]ClO_4 \cdot 0.5bipy$, $[^{99}Tc(phen)(CO)_3(CNAd)]ClO_4$, $[Re(bipy)(CO)_3(CNAd)]ClO_4 \cdot 0.5bipy$, and $[Re(phen)(CO)_3(CNAd)]ClO_4$ was determined by single crystal X-ray diffraction. As shown by EDA-NOCV, CNAd exhibits lower, compared to CO, π-acceptor power in the complex $[^{99}Tc(bipy)(CO)_3(CNAd)]^+$ and preserves the σ-donor power, which agrees with the high-frequency shift of the ν(CN) IR band of the ligand upon coordination.

Keywords: technetium, rhenium, tricarbonyl complexes, adamantane, IR spectroscopy, DFT

DOI: 10.1134/S1066362226050085

INTRODUCTION

Adamantane is widely used in the design of biologically active molecules because its moiety improves the pharmacokinetic and pharmacodynamic properties [1, 2]; in particular, it makes the compound appreciably more lipophilic [3, 4]. Because of high chemical stability, resistance to oxidation, relatively small size, and low toxicity, adamantane is a promising component of systems for targeted drug delivery. One of effective approaches to intracellular delivery of proteins and liposomes is based on the host–guest supramolecular interaction in which the adamantane label on the protein or liposome surface acts as a guest ensuring supramolecular binding with β-cyclodextrin modified with the peptide penetrating into the cell [5].

This approach, in principle, can also be used in nuclear medicine for targeted delivery of technetium-99*m* and rhenium (including the stable and radioactive (^{186}Re, ^{188}Re) isotopes) complexes [6, 7]. Introduction of an adamantyl-containing ligand into the coordination sphere of these metals creates a "bridge" between the metal complex and cyclodextrin–peptide vector. The *fac*-tricarbonyl core *fac*-$[M(CO)_3]^+$ (M = ^{99m}Tc, Re) ensuring high inertness and stability of the complexes in vivo can serve as a base for designing such complexes [8].

The adamantyl moiety can be introduced into the coordination sphere via isocyanide group using 1-adamantyl isocyanide (CNAd). Like carbonyl groups, this ligand is a strong π-acceptor and stabilizes the metal in oxidation state +1. To complete the coordination

sphere in accordance with the "2 + 1" approach, it is appropriate to use stable bidentate NN-donor ligands such as 2,2'-bipyridine (bipy) and 1,10-phenanthroline (phen) [9, 10]. An important advantage of using NN-aromatic diimines is associated with the fact that the corresponding rhenium complexes exhibit photophysical properties suitable for photodynamic therapy [11] and are highly cytotoxic [12, 13]. With the adamantane moiety introduced into an NN-bidentate ligand, rhenium *fac*-tricarbonyl complexes are active in photodecarbonylation and photosensitization [14, 15]. Thus, the suggested approach shows promise for the development of theranostic agents of new generation, based on a combination of technetium-99*m* with stable rhenium or rhenium-186/188. This study was aimed at introducing the adamantyl fragment into the coordination sphere of technetium(I) and rhenium(I) by preparing the "2 + 1" tricarbonyl complexes $[M(NN)(CO)_3(CNAd)]^+$ (M = ^{99}Tc, Re).

EXPERIMENTAL

Caution! Compounds of technetium-99 ($T_{1/2} = 2.11 \times 10^5$ years, $E_{\beta max} = 293.8$ keV) are radioactive and should be handled only in specially equipped and certified laboratories.

$[^{99}TcBr(CO)_5]$ was prepared by autoclave carbonylation of $K[^{99}TcO_4]$ with a mixture of formic and hydrobromic acids at 170°C for 2 h [16]. The complex can also be prepared at atmospheric pressure by the procedure that we developed previously [17]. Prior to use, $[^{99}TcBr(CO)_5]$ was additionally purified by sublimation in a rough vacuum. Silver perchlorate was prepared by precipitation of silver carbonate from an aqueous solution of silver nitrate with sodium carbonate, followed by dissolution of the precipitate in concentrated perchloric acid and drying in a vacuum at 50–60°C. $[^{99}Tc(ClO_4)(CO)_5]$ was prepared by stirring $[^{99}TcBr(CO)_5]$ with excess $AgClO_4$ in dichloromethane at room temperature in the dark for 1 h [18]. $[ReCl(CO)_5]$ was prepared by carbonylation of K_2ReCl_6 with a mixture of formic and hydrochloric acids at 180°C and a pressure of 120 atm, followed by vacuum sublimation of the product. All the other chemicals were purchased from Sigma–Aldrich and used without additional purification. Dichloromethane was distilled from P_2O_5.

The IR spectra of the liquid samples were recorded with a Simex FT-801 spectrometer in the range 1700–2300 cm^{-1} using CaF_2 cells. The NMR spectra were recorded at 298 K with a Bruker 400 Avance spectrometer operating at 400 MHz for ^{1}H and 90 MHz for ^{99}Tc. The ^{99}Tc chemical shifts are given relative to potassium pertechnetate in H_2O–D_2O.

The crystal structures of four complexes were determined by single crystal X-ray diffraction (SCXRD) analysis. The crystals were fixed on cryoloops. The diffraction data were collected on a Rigaku Oxford Diffraction XtaLAB Synergy S diffractometer using monochromated microfocused CuK_α radiation. The absorption correction was introduced in the CrysAlisPro program complex [19]. The structures were solved using the Intrinsic Phasing algorithm and were refined using the SHELX programs [20, 21] integrated in the OLEX2 program package [22]. The final models included the coordinates and anisotropic parameters of atomic shifts for all nonhydrogen atoms. The hydrogen atoms bonded to carbon atoms were placed in geometrically calculated positions and were included in the refinement using the rider model with the thermal parameters U_{iso}(H) equal to $1.2U_{eq}$(C) and bond lengths C_{ar}–H 1.083 Å, C_{sp2}–H 1.077 Å [23]. The crystallographic data are given in Supplementary Information, Table S1.

Synthesis of 1-adamantyl isocyanide (CNAd). CNAd was prepared by the adapted procedure [24] from 1-adamantylamine by its conversion to *N*-adamantylformamide, followed by dehydration with $POCl_3$ in Et_3N. Colorless crystals; yield 84%. The ^{1}H NMR spectrum of the compound prepared fully agrees with the published data [25].

Synthesis of $[Tc(bipy)(CO)_3(CNAd)]ClO_4$ (1a). Weighed portions of $[^{99}Tc(ClO_4)(CO)_5]$ (34 mg, 0.10 mmol) and 2,2'-bipyridine (50 mg, 0.323 mmol) were placed in a penicillin vial, 4 mL of ethanol was added, and the mixture was stirred at 60°C for 6 h. Within 30 min, the reaction mixture turned yellow [18, 26]. A weighed portion of 1-isocyanoadamantane (17 mg, 0.108 mmol) dissolved in 1 mL of ethanol on heating to 60°C was added. The mixture was stirred at 60°C for 10 h. The solution was left in a non-tightly closed penicillin vial at room temperature in the dark to allow the solvent to evaporate. Yellowish crystals suitable for SCXRD were formed on the bottom of the vial. Yield 72% (50 mg, 0.084 mmol). IR spectrum (EtOH), ν, cm^{-1}: 2194 w (C≡N), 2052 s (C≡O), 1983 s (C≡O), 1953 s (C≡O). ^{99}Tc NMR spectrum (CD_3CN, 298 K), δ, ppm: –1276.04. The SCXRD analysis showed that the product

had the composition **1a**·0.5bipy. Crystallographic data: monoclinic system, space group $P2_1/n$; a = 15.1962(4), b = 6.4569(2), c = 28.9916(7) Å, β = 99.829(2)°, V = 2802.91(13) Å^3, Z = 4; R_1 = 3.62%. CCDC 2586723.

Synthesis of [Tc(phen)(CO)$_3$(CNAd)]ClO$_4$ (2a). Weighed portions of [^{99}Tc(ClO$_4$)(CO)$_5$] (14 mg, 0.041 mmol) and 1,10-phenanthroline (19 mg, 0.103 mmol) were placed in a penicillin vial, 4 mL of ethanol was added, and the mixture was stirred at 60°C for 6 h. The mixture turned yellow within 30 min [18, 26]. A weighed portion of 1-isocyanoadamantane (7 mg, 0.042 mmol) dissolved in 1 mL of ethanol at 60°C was added. The mixture was stirred at 60°C for 15 h. The solution was left in a non-tightly closed penicillin vial at room temperature in the dark to allow the solvent to evaporate. Dark yellow crystals were formed on the bottom of the vial. Yield 93% (24 mg, 0.038 mmol). IR spectrum (EtOH), ν, cm^{-1}: 2194 w (C≡N), 2053 s (C≡O), 1984 s (C≡O), 1956 s (C≡O). ^{99}Tc NMR spectrum (CD$_3$CN, 298 K), δ, ppm: –1284.05. Crystallographic data for **2a**: monoclinic system, space group $P2_1/n$; a = 12.4140(3), b = 25.6045(5), c = 16.3767(6) Å, β = 104.430(3)°, V = 5041.2(3) Å^3, Z = 8; R_1 = 13.6%. CCDC 2586724.

Synthesis of [Re(bipy)(CO)$_3$(CNAd)]ClO$_4$ (1b). To a weighed portion of [ReCl(CO)$_5$] (30 mg, 0.083 mmol), we added AgClO$_4$ (130 mg, 0.482 mmol) and 4 mL of CH$_2$Cl$_2$. The mixture was stirred for 24 h in the dark and filtered through a fiber glass filter; the solvent was removed on a rotary evaporator. The [Re(ClO$_4$)(CO)$_5$] thus obtained (35 mg, 0.082 mmol) was dissolved in 3 mL of ethanol, and 1 mL of a solution of 2,2'-bipyridine (13 mg, 0.082 mmol) in ethanol was added. The mixture was heated at 60°C for 2 h. The resulting yellow solution was evaporated on a rotary evaporator, 3 mL of CH$_2$Cl$_2$ was added, and the solution was evaporated again; the procedure was repeated until a dry crystalline residue was obtained. The dry residue was washed with three 2-mL portions of hexane and was dried on a rotary evaporator. The [Re(bipy)(CO)$_3$(ClO$_4$)] thus obtained was dissolved in 2 mL of ethanol, 1 mL of a solution of CNAd (15 mg, 0.092 mmol) in ethanol was added, and the mixture was heated at 60°C for 24 h. [Re(bipy)(CO)$_3$(CNAd)]ClO$_4$ was purified by column chromatography; the impurities were eluted with CH$_2$Cl$_2$, and the product was eluted with ethanol. The yield of **1b** was 47% (22 mg, 0.038 mmol). IR spectrum (EtOH), ν, cm^{-1}: 2195 w (C≡N), 2041 s (C≡O), 1967 s (C≡O), 1942 s (C≡O). ^{1}H NMR (298 K, CDCl$_3$, δ, ppm): 8.95 (d, ^3J = 4 Hz, 2H), 8.90 (d, ^3J = 8 Hz, 2H), 8.42 (t, ^3J = 8 Hz, 2H), 7.73 (t, ^3J = 8 Hz, 2H), 2.09–2.04 (m, 3H), 1.85–1.81 (m, 6H), 1.60 (t, ^3J = 16 Hz, 6H). To obtain single crystals of **1b**, about 2 mg of bipy was added to an ethanol solution of **1b** purified by column chromatography (we failed to obtain single crystals without excess bipy). The crystals obtained by recrystallization of **1b** from EtOH in the presence of 2,2'-bipyridine appeared to be suitable for SCXRD. Similarly to the Tc analog, the single crystal had the composition **1b**·0.5bipy. Crystallographic data: monoclinic system, space group $P2_1/n$; a = 15.1414(7), b = 6.4666(3), c = 29.0133(14) Å, β = 100.220(5)°, V = 2795.7(2) Å^3, Z = 4; R_1 = 4.01%. CCDC 2586725.

Synthesis of [Re(phen)(CO)$_3$(CNAd)]ClO$_4$ (2b). To a weighed portion of [ReCl(CO)$_5$] (33 mg, 0.092 mmol), we added AgClO$_4$ (175 mg, 0.842 mmol) and 4.5 mL of CH$_2$Cl$_2$. The mixture was stirred for 5 h in the dark. After that, the mixture was filtered through a fiber glass filter and evaporated on a rotary evaporator. To [Re(ClO$_4$)(CO)$_5$] thus obtained (28 mg, 0.066 mmol), a weighed portion of 1,10-phenanthroline (12 mg, 0.066 mmol) and 3 mL of ethanol were added. The mixture was heated at 70°C for 1 h. A weighed portion of CNAd (11 mg, 0.066 mmol) was added, and the mixture was heated for 24 h at 60°C. The product was purified by recrystallization from hot ethanol, and the crystals formed were filtered off, washed with ethanol, and dried in a vacuum. The crystals obtained by recrystallization of **2b** from hot ethanol were suitable for SCXRD. Yield 35% (16 mg, 0.023 mmol). IR spectrum (EtOH), ν, cm^{-1}: 2193 w (C≡N), 2043 s (C≡O), 1970 m (C≡O), 1943 m (C≡O). ^{1}H NMR (298 K, CDCl$_3$, δ, ppm): 9.35 (dd, ^3J = 5.2, ^4J = 1.4 Hz, 2H), 8.95 (dd, ^3J = 8.3, ^4J = 1.4 Hz, 2H), 8.35 (s, 2H), 8.11 (dd, ^3J = 8.3, ^3J = 5.1 Hz, 2H), 2.01 (m, 3H), 1.77 (d, J = 2.9 Hz, 6H), 1.55–1.59 (m, 3H). ^{1}H NMR (298 K, CD$_3$CN, δ, ppm): 9.42 (dd, ^3J = 5.1, ^4J = 1.4 Hz, 2H), 8.88 (dd, ^3J = 8.3, ^4J = 1.4 Hz, 2H), 8.27 (s, 2H), 8.06 (dd, ^3J = 8.3, ^3J = 5.2 Hz, 2H), 1.92–1.91 (m, 3H), 1.63 (d, ^3J = 3.0 Hz, 6H), 1.57–1.53 (m, 3H), 1.50–1.43 (m, 3H). Crystallographic data for **2b**: monoclinic system, space group $P2_1/n$; a = 12.39377(10), b = 25.5738(2), c = 16.35409(15) Å, β = 103.9241(9)°, V = 5031.21(8) Å^3, Z = 4; R_1 = 2.88%. CCDC 2586726.

COMPUTATION

The DFT calculations with full geometry optimization were performed with the ORCA 6.1 program [27]

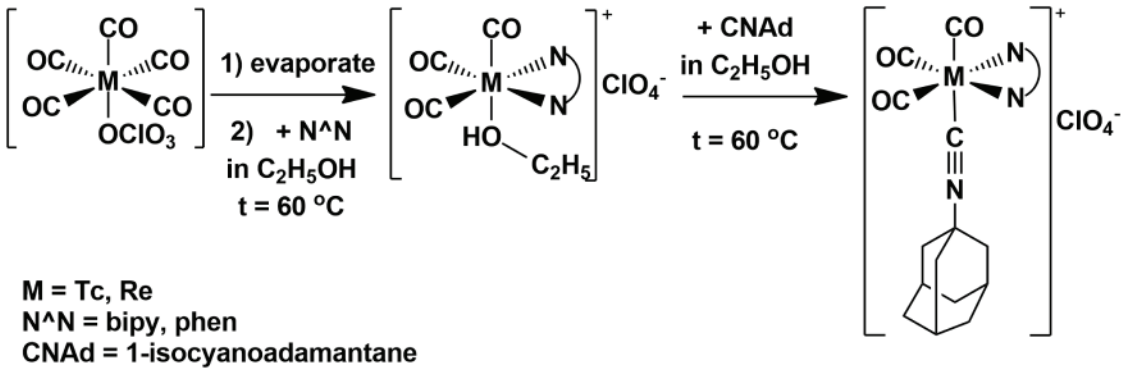


Fig. 1. Scheme of the synthesis of *fac*-[M(NN)(CO)$_3$(CNAd)] (NN = bipy, phen; M = ^{99}Tc, Re).

using the TPSSh functional [28, 29], D3 correction for variance [30] with zero damping, jorge-TZP-ZORA basis set [31, 32] in combination with the resolution of identity algorithm [33], and auxiliary basis sets generated by the AutoAux method [34]. The zero-order regular approximation (ZORA) was used for taking into account relativistic effects [35–38]. Tight convergence criteria (TightOpt; TightSCF) were used in the geometry optimization and self-consistent field calculations. The conductor-like polarizable continuum model (CPCM) [39] was used for taking into account the solvent in the implicit form. In all the cases, the normal mode analysis revealed no imaginary frequencies. The AIM charge calculations [40] were performed using the Multiwfn 3.8 program [41]. The AIM charges were calculated using the lunatic quality grid to construct electron density basins and integrate the density around atomic centers and uniform grids with accurate refinement of basin boundaries. The EDA-NOCV (energy decomposition analysis of natural orbitals for chemical valence) calculations for the complexes $[Tc(bipy)(CO)_3(CNAd)]^+$ and $[Tc(bipy)(CO)_4]^+$ were performed with the ORCA 6.1 program on the TPSSh-D3zero/jorge-TZP-ZORA theory level using the geometries optimized on the same level. We performed the fragmentation of $[Tc(bipy)(CO)_3(CNAd)]^+$ into the fragments $[Tc(bipy)(CO)_3]^+$ and CNAd and of $[Tc(bipy)(CO)_4]^+$ into $[Tc(bipy)(CO)_3]^+$ and CO with the multiplicity of 1 for each fragment. To analyze NOCV pairs, ETS-NOCV calculations were additionally performed with the Multiwfn 3.8 program on the same level of theory. The deformation density $\Delta\rho_i$ was visualized with the ChemCraft 1.8 program [42] at the following isosurface values (CV): $CV(E_{orb1}) = 0.01$, $CV(E_{orbi}) = 0.005$ ($i = 2, 3$). The color code of the charge flow for $\Delta\rho_i$ is blue → red.

RESULTS AND DISCUSSION

To develop a new approach to targeted delivery of diagnostic and therapeutic agents based on technetium and rhenium complexes, we prepared tricarbonyl derivatives with 2,2'-bipyridine (bipy) and 1,10-phenanthroline (phen) in combination with 1-adamantyl isocyanide (CNAd). We used long-lived ^{99}Tc as a chemical analog of diagnostic ^{99m}Tc and natural rhenium. The complexes were prepared from the precursors $[M(ClO_4)(CO)_5]$ (M = ^{99}Tc, Re) by a two-step procedure used previously for preparing other "2 + 1" tricarbonyl complexes of these elements [10, 26, 43, 44] (Fig. 1).

In the first step, bidentate NN-aromatic diimine was introduced into the coordination sphere by heating a mixture of $[M(ClO_4)(CO)_5]$ with the corresponding ligand in ethanol. Then, the coordinated solvent molecule in the intermediate tricarbonyl complex $[M(NN)(CO)_3(EtOH,H_2O)]$ was replaced by 1-adamantyl isocyanide. The target products $[^{99}Tc(NN)(CO)_3(CNAd)]ClO_4$ (NN = bipy (**1a**), phen (**2a**)) and $[Re(NN)(CO)_3(CNAd)]ClO_4$ (NN = bipy (**1b**), phen (**2b**)) were isolated in good yields for Tc (70–90%) and moderate yields for Re (30–50%). The lower yields of rhenium complexes are probably caused by higher inertness of Re(I) complexes, compared to Tc(I), in ligand replacement, which requires longer heating and additional chromatographic purification.

The IR spectra of **1a**, **1b**, **2a**, and **2b** in EtOH have characteristic absorption bands in the range of CO stretches (Fig. 2; Supplementary Information, Figs. S9,

S14), which corresponds to the *fac*-configuration of the tricarbonyl moiety.

The ν(CO) bands in the spectra of **1a** and **2a** are close in position to those in the spectra of $[^{99}Tc(bipy)(CO)_3(CNCH_2COOEt)]ClO_4$ and $[^{99}Tc(phen)(CO)_3(CNCH_2COOEt)]ClO_4$, which indicates that the influence of the substituent at the isocyanide group on the manifestation of the *trans* effect is weak [26]. On the other hand, comparison of the IR spectrum of *fac*-$[Re(bipy)(CO)_3(CNAd)]^+$ (ν(CO) 2041, 1963, 1936 cm^{-1}) with that of *fac*-$[Re(bipy)(CO)_3(PPh_3)]^+$ (ν(CO) 2041, 1954, 1924 cm^{-1}) in acetonitrile [45] shows that the π-acceptor power of CNAd is higher because the replacement of PPh_3 by CNAd leads to the high-frequency shift of the low-frequency and middle ν(CO) bands (Supplementary Information, Fig. S10).

The CN stretching vibration band (**1a**, 2194; **2a**, 2194; **1b**, 2195; **2b**, 2193 cm^{-1}) has low intensity and complex shape suggesting the Fermi resonance or the presence of several conformations. The ν(CN) band in the spectra of the complexes is shifted toward higher frequencies relative to free CNAd (2130 cm^{-1}), which suggests strengthening of the C≡N bond upon coordination. This is due to the prevalence of the σ-donor power of the isocyanide ligand over it π-acceptor power [46, 47]. It is interesting that, in the tetrakis-isocyanide complexes $[^{99}Tc(NN)(CNR)_4]PF_6$ (R = *t*-Bu, Me, *m*-Xyl), on the contrary, the ν(CN) band is shifted toward lower frequencies by 7–39 cm^{-1} [48].

To compare the σ-donor and π-acceptor power of 1-adamantyl isocyanide with that of the carbonyl ligand, we performed an EDA-NOCV calculation with the fragmentation into the $[Tc(bipy)(CO)_3]^+$ and L moieties, where L = CNAd or CO. The EDA results are given in Table 1.

The interaction energy with the isocyanide ligand is higher than with the carbonyl ligand, which agrees with the reactivity: The $[^{99}Tc(bipy)(CO)_4]^+$ cation has not yet be obtained. The larger interaction energy ΔE_{int} is ensured by the electrostatic contribution

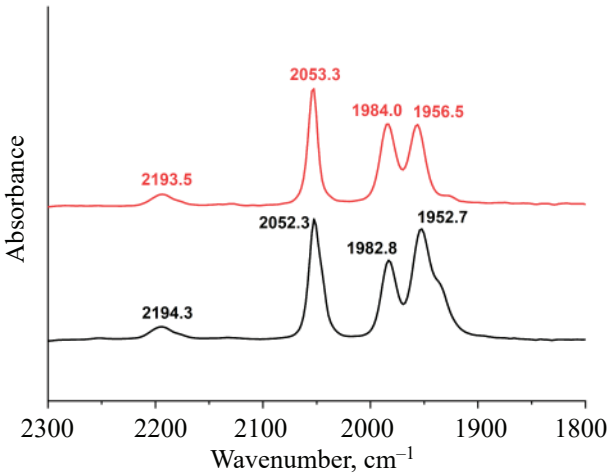


Fig. 2. IR spectra of $[^{99}Tc(bipy)(CO)_3(CNAd)]ClO_4$ (1a, black) and $[^{99}Tc(phen)(CO)_3(CNAd)]ClO_4$ (2a, red) in EtOH.

ΔE_{elstat} and is due to the negative charge on the carbon atom in the CN group [49]. According to the NOCV analysis, the σ-donor power of 1-adamantyl isocyanide is practically identical to that of the carbonyl ligand, whereas the π-acceptor power of the former is appreciably weaker (Fig. 3). This fact accounts for the absence of the bathochromic shift of ν(CN) in the IR spectrum in going from noncoordinated CNAd to $[^{99}Tc(bipy)(CO)_3(CNAd)]ClO_4$.

The lower π-acceptor power of the isocyanide ligand is also confirmed by calculating QTAIM charges on the ligands. The total charge on CNAd in the complex is weakly positive and equal to 0.06 a.u., whereas CO withdraws the electron density and acquires a negative charge of –0.14. The QTAIM charge on the technetium atom is approximately equal in both complexes: 1.40 and 1.41 in $[Tc(bipy)(CO)_3(CNAd)]^+$ and $[Tc(bipy)(CO)_4]^+$, respectively. Thus, the strength of the C–O and C–N bonds is confirmed by the balance between strengthening of the bond due to σ-donation and its loosening due to back π-donation upon coordination to the metal.

Table 1. EDA results for the $[Tc(bipy)(CO)_3]^+$ and L fragments on the TPSSh-D3zero/jorge-TZP-ZORA theory level. All the values are given in kcal/mol

Fragments	ΔE_{int}	ΔE_{orb}[a]	ΔE_{elstat}[a]	ΔE_{disp}[a]	ΔE_{Pauli}
$[Tc(bipy)(CO)_3]^+$ + CNAd	–59.26	–62.69 (36.6%)	–105.37 (61.6%)	–3.09 (1.8%)	111.9
$[Tc(bipy)(CO)_3]^+$ + CO	–43.87	–74.80 (45.9%)	–86.60 (53.2%)	–1.48 (0.9%)	119.02

[a] The contribution of the component to the total attractive interaction of the fragments, $\Delta E_{elstat} + \Delta E_{orb} + \Delta E_{disp}$, is given in parentheses.

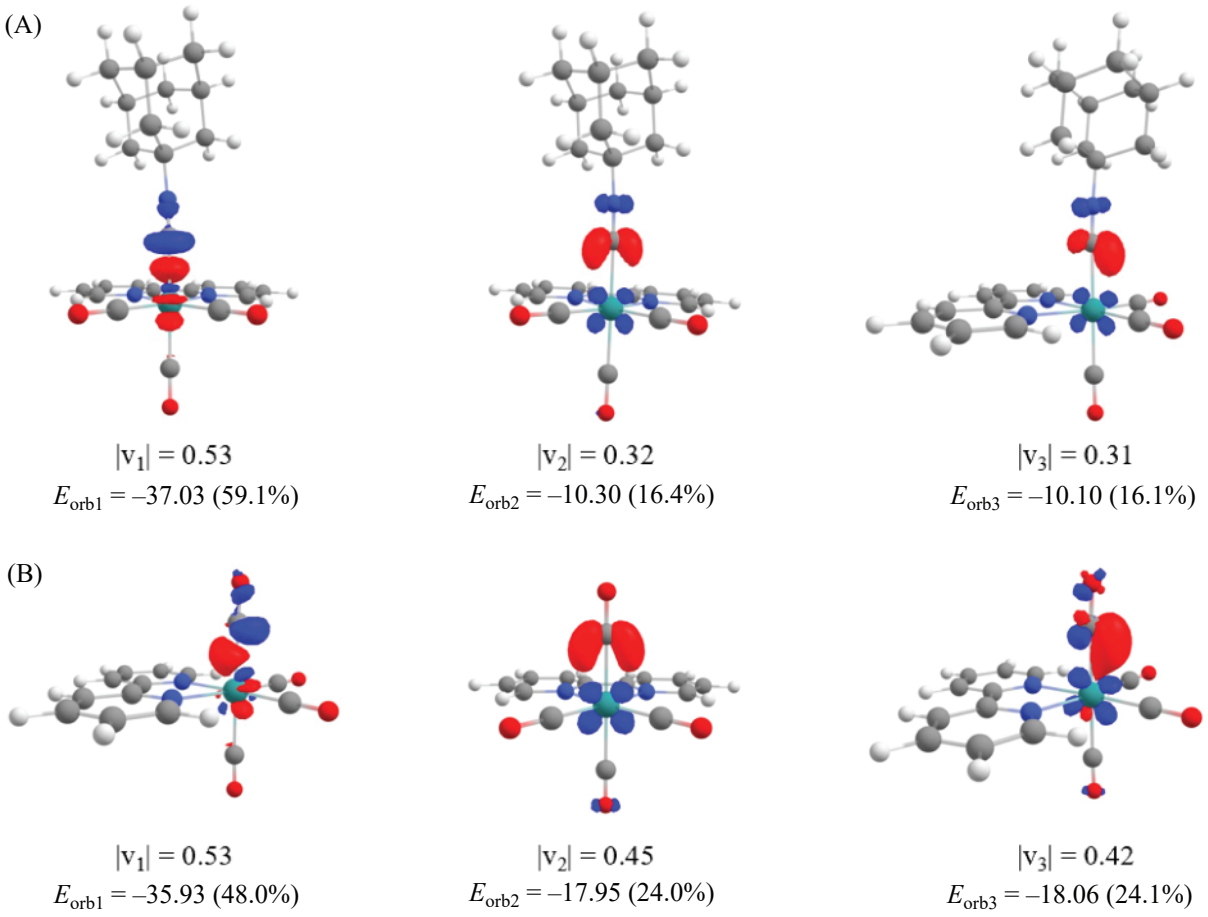


Fig. 3. Maps of the deformation density $\Delta\rho_i$ for the first three pairwise orbital interactions in $[Tc(bipy)(CO)_3(L)]^+$ (L = CNAd, CO), obtained using the fragments $[Tc(bipy)(CO)_3]^+$ and L in the singlet electronic state. Calculations on the TPSSh-D3zero/jorge-TZP-ZORA theory level. (A) $[Tc(bipy)(CO)_3(CNAd)]^+$ and (B) $[Tc(bipy)(CO)_4]^+$. The energies are given in kcal/mol. The contribution of the given interaction to ΔE_{orb} is given in parentheses.

The broadening of the CN vibration band in the IR spectra of complexes **1a**, **1b**, **2a**, and **2b** may be due to several factors. Previously, our research group showed by DFT calculations that the absorption band in the region of CN stretches in $[M(CO)_5(CNCH_2COOEt)]ClO_4$ (M = ^{99}Tc, Re) is a band of mixed CN and CO vibrations [50]. To study such behavior in the *fac*-tricarbonyl complexes, we calculated by DFT the IR frequencies for $[^{99}Tc(bipy)(CO)_3(CNAd)]^+$ and free CNAd. The experimental IR spectrum of the free ligand in EtOH differs from the calculated spectrum in the number of bands in the region of C≡N stretches (Table 2; Supplementary Information, Fig. S20).

At the same time, both the calculated and experimental IR spectrum of a solution of CNAd in nonpolar aprotic CCl_4 has a single absorption band in the region of CN stretches (experimental frequency 2130 cm^{-1}; Supplementary Information, Fig. S19, Table S19). Such difference is caused by the formation of hydrogen bonds between the CN group and OH group of ethanol in the solution. The formation of hydrogen bonds between isocyanides and protic solvents was shown previously [52]. Because the calculation was performed with taking into account the solvent in the implicit form (CPCM), the formation of hydrogen bonds between the CN group and solvent was not taken into account; therefore, there is a single C≡N stretching band in the calculated spectrum.

Calculation of the frequencies for $[Tc(bipy)(CO)_3(CNAd)]^+$ also gives a single absorption band in the region of C≡N stretches (Table 1). The calculated CN frequency in the complex has a minimal contribution of CO vibrations. The calculated CO

Table 2. Experimental and calculated (TPSSh-D3ZERO/jorge-TZP-ZORA CPCM(EtOH)) ν(CO) and ν(CN) frequencies, cm^{-1}

Compound	ν(CO), cm^{-1}		ν(CN), cm^{-1}	
	experimental	calculated	experimental	calculated
CO	2136 [51]	2180		
CNAd			2130 2143 2160	2193
$[^{99}Tc(bipy)(CO)_3(CNAd)]ClO_4$[a]	2052 1983 1953	2062 1978 1952	2194	2254

[a] The calculated frequencies are given for $[Tc(bipy)(CO)_3(CNAd)]^+$.

stretching frequencies well agree with the experimental values. The slight broadening of the C≡N band in the complex may be caused by the formation of π-type hydrogen bonds [53] and by the conformational mobility of the fragment of the isocyanide ligand. The latter assumption is supported by a change in the N(bipy)–Tc–C(Ad) angle in going from the structure optimized in a vacuum (91.5°) to the structure optimized with taking into account ethanol in the implicit form (81.8°) (Fig. 4).

The ^{99}Tc NMR signals of $[^{99}Tc(bipy)(CO)_3(CNAd)]ClO_4$ (**1a**) and $[^{99}Tc(phen)(CO)_3(CNAd)]ClO_4$ (**2a**) are observed at –1276.04 and –1284.05 ppm, respectively, i.e., in the higher field compared to $[^{99}TcBr(phen)(CO)_3]$ (–1085.35 ppm in CD_2Cl_2) [54]. This fact agrees with the previously revealed trends for technetium-99 carbonyl complexes. For example, in the series $[^{99}TcBr(CO)_5]$–$[^{99}Tc(acac)(CO)_4]$–$[^{99}Tc(acac)(CO)_3(PPh_3)]$–$[^{99}Tc(acac)(CO)_2(PPh_3)_2]$, the chemical shift increases from –1802 to –891 ppm [55, 56] upon replacement of strong π-acceptor CO ligands by less strong π-acceptors PPh_3. On the other hand, the ^{99}Tc NMR signal of the complex $[^{99}Tc(bipy)(CO)_3(CNAd)]ClO_4$ (**1a**) (–1276.04 ppm) is slightly shifted downfield compared to the signal of its phenanthroline analog **2a**. This fact is most likely due to stronger π-acceptor power of the phenanthroline ligand.

All the complexes obtained were characterized by single crystal X-ray diffraction. Compounds **1a**, **1b**, **2a**, and **2b** crystallize in the monoclinic system, space group $P2_1/n$ (no. 14). Figure 5 shows the molecular structures of the complex cations. The crystallographic data are given in Supplementary Information, Table S1.

Single crystals of **1a** and **1b** could be obtained only in the presence of excess 2,2′-bipyridine, which was

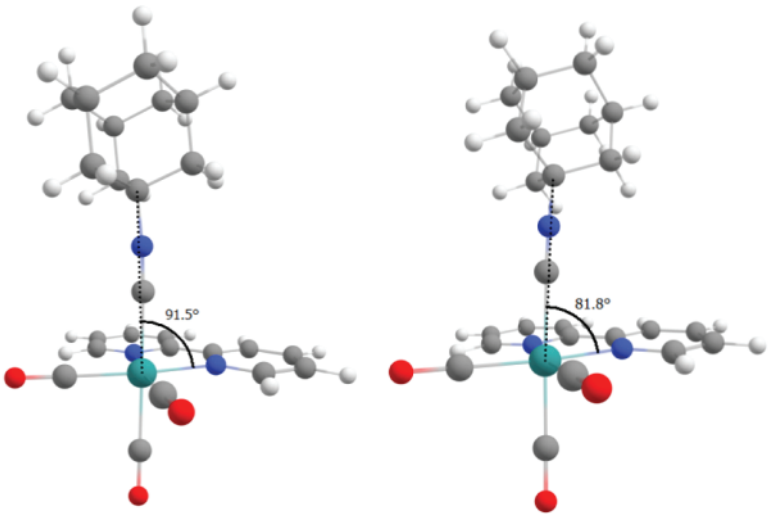


Fig. 4. Optimized structure of the $[Tc(bipy)(CO)_3(CNAd)]^+$ cation in a vacuum (left) and with taking into account ethanol in the implicit form (right), calculated on the TPSSh-D3zero/jorge-TZP-ZORA level of theory.

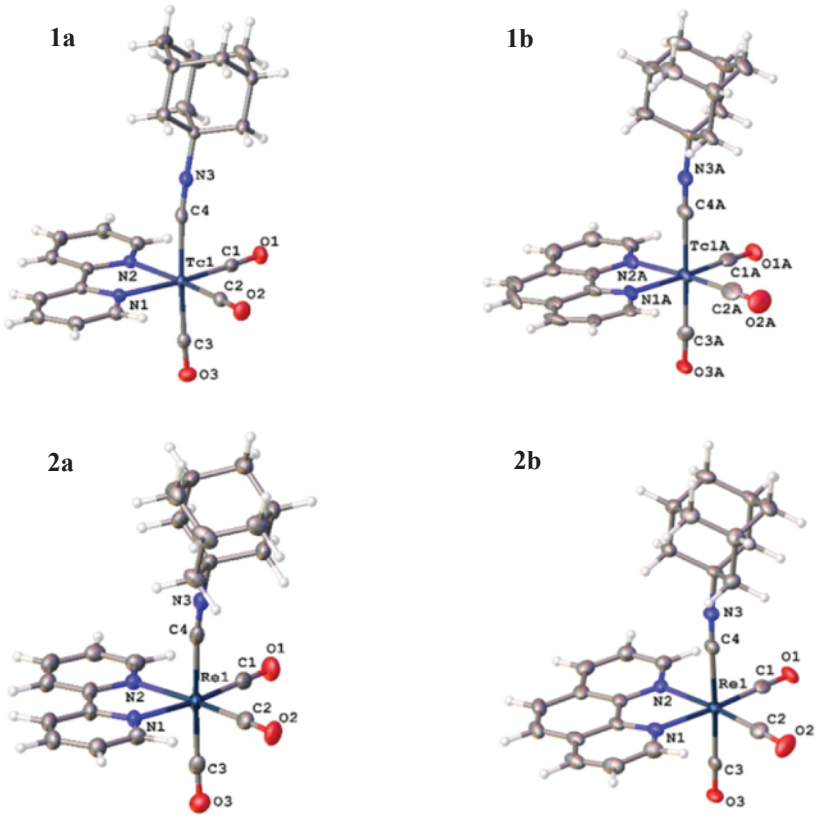


Fig. 5. Molecular structure of $[^{99}Tc(bipy)(CNAd)(CO)_3]^+$ in **1a**·0.5bipy, $[^{99}Tc(bipy)(CNAd)(CO)_3]^+$ in **2**a, $[Re(bipy)(CO)_3(CNAd)]^+$ in **1b**·0.5bipy, and $[Re(phen)(CO)_3(CNAd)]^+$ in **2b**.

incorporated into the crystal structure. Compounds **2a** and **2b** crystallized from hot ethanol without additional agents. No directional noncovalent interactions between outer-sphere bipyridine molecules and complex cations were revealed. In all the crystal structures of both technetium and rhenium complexes, perchlorate ions are bound to metal complex cations via weak hydrogen bonds with protons of diimine and adamantane ligands (Supplementary Information, Figs. S4, S8, S13, S18).

In all the structures, ∠(M–C–N) and ∠(C–N–C) deviate from 180°, which is probably caused by the above-discussed conformational mobility of the M–C–N–C fragment (Table 3).

In the structures of **1a** and **2b**, the M–CO_{ax} bond in the *trans* position to CNAd is longer by ~0.03 Å than the M–CO_{eq} bond, whereas in the structures of **1b** and **2a** all the three M–C bonds are equivalent. The Tc–N bond lengths in **1a** (2.1657(19) and 2.1739(18) Å) and **2a** (2.179(12) and 2.194(11) Å) coincide with those in $[^{99}Tc(bipy)(CO)_3(CNCH_2COOEt)]ClO_4$ (2.179(2) and 2.175(2) Å) and $[^{99}Tc(phen)(CO)_3(CNCH_2COOEt)]ClO_4$ (2.175(3) and 2.183(3) Å) [26]. On the other hand, the Tc–C(N) bond length in **1a** (2.109(2) Å) is larger than that in $[^{99}Tc(bipy)(CO)_3(CNCH_2COOEt)]ClO_4$ (2.084(3) Å), which suggests weaker π-acceptor properties of CNAd compared to $CNCH_2COOEt$. The C≡O bond length in the *trans* position to CNAd

Table 3. Values of ∠(M–C–N) and ∠(C–N–C) in the structures of **1a**, **2a**, **1b**, and **2b**

Angle	**1a**	**2a**	**1b**	**2b**
∠(M–C–N)	171.2(2)°	174.3(12)°	172.0(4)°	177.8(4)°
∠(C–N–C)	174.0(2)°	178.7(14)°	173.1(5)°	177.7(4)°

in **1a** (1.139(3) Å) is practically the same as that in [^{99}Tc(bipy)(CO)$_3$(CNCH$_2$COOEt)]ClO$_4$ (1.140(3) Å), which is consistent with the IR data. It is interesting that, in [Re(phen)(CO)$_3$(CNAd)]ClO$_4$ (**2b**), the Re–C$_{transCNAd}$ (1.963(4) Å) and C≡O$_{transCNAd}$ (1.135(4) Å) bond lengths are close to the Re–C$_{transPPh3}$ (1.949(5) Å) and C≡O$_{transPPh3}$ (1.128(6) Å) bond lengths in [Re(phen)(CO)$_3$(PPh$_3$)]OTf [57]. The bond lengths and angles are given in the Supplementary Information.

CONCLUSIONS

Technetium-99 and rhenium *fac*-tricarbonyl complexes [M(NN)(CO)$_3$(CNAd)]ClO$_4$ (NN=bipy, phen), in which the adamantyl moiety is introduced into the coordination sphere via isocyanide group, have been prepared and characterized. The complexes are stable in an ethanol solution.

The IR spectra of the compounds prepared exhibit the following characteristic features. The high-frequency shift of the ν(CN) band of coordinated 1-adamantyl isocyanide relative to noncoordinated CNAd is due to weak π-acceptor power of CNAd. This conclusion is confirmed by the results of EDA-NOCV analysis. The broadening of the ν(CN) band in the spectra of the complexes, according to the results of DFT calculations and comparison of the spectra in different solvents, can be attributed to the conformational mobility of the adamantyl substituent and formation of π-type hydrogen bonds in ethanol solutions of the complexes.

The complexes prepared are convenient models for developing the chemistry of ^{99m}Tc and rhenium radioisotopes (^{186}Re, ^{188}Re) and open prospects for the development of theranostic agents using the adamantane–cyclodextrin supramolecular delivery system.

FUNDING

The study was financially supported by the Russian Science Foundation (project no. 26-13-00356, https://rscf.ru/project/26-13-00356/).

ACKNOWLEDGMENTS

The authors are grateful to the resource centers for magnetic resonance investigation methods and for X-ray diffraction investigation methods of the Science Park of the St. Petersburg State University.

CONFLICT OF INTEREST

The authors declare that they have no conflicts of interest.

SUPPLEMENTARY INFORMATION

The Supplementary Information to this paper (spectra, crystallographic data, structural details) are available to authorized users at https:/doi.org/ 10.1134/S1066362226050085.

REFERENCES

1. Dragomanova, S. and Andonova, V., *PHAR*, 2023, vol. 70, no. 4, pp. 1057–1066.
https://doi.org/10.3897/pharmacia.70.e111593
2. Dane, C., Cumbers, G.A., Allen, B., Montgomery, A.P., Danon, J.J., and Kassiou, M., *Aust. J. Chem.*, 2024, vol. 77, no. 8, ID CH24075.
https://doi.org/10.1071/CH24075
3. Wanka, L., Iqbal, K., and Schreiner, P.R., *Chem. Rev.*, 2013, vol. 113, no. 5, pp. 3516–3604.
https://doi.org/10.1021/cr100264t
4. Chochkova, M., Georgieva, A., Ilieva, T., Andreeva, M., Pramatarov, G., Petek, N., Petrova, P., Štícha, M., Mitrev, Y., and Svete, J., *J. Chem.*, 2022, vol. 2022, pp. 1–11.
https://doi.org/10.1155/2022/7582587
5. Kitagishi, H., Jiromaru, M., and Hasegawa, N., *ACS Appl. Bio Mater.*, 2020, vol. 3, no. 8, pp. 4902–4911.
https://doi.org/10.1021/acsabm.0c00421
6. Currie, G.M. and Rohren, E.M., *Semin. Nucl. Med.*, 2025, vol. 55, no. 5, pp. 829–840.
https://doi.org/10.1053/j.semnuclmed.2025.01.005
7. Bauer, E.B., Haase, A.A., Reich, R.M., Crans, D.C., and Kühn, F.E., *Coord. Chem. Rev.*, 2019, vol. 393, pp. 79–117.
https://doi.org/10.1016/j.ccr.2019.04.014
8. Alberto, R., Schibli, R., Waibel, R., Abram, U., and Schubiger, A.P., *Coord. Chem. Rev.*, 1999, vol. 190–192, pp. 901–919.
https://doi.org/10.1016/S0010-8545(99)00128-9
9. Miroslavov, A.E., Sakhonenkova, A.P., Tyupina, M.Yu., and Sidorenko, G.V., *Russ. J. Gen. Chem.*, 2023, vol. 93, no. 2, pp. 327–331.
https://doi.org/10.1134/S1070363223020135
10. Tyupina, M.Yu., Miroslavov, A.E., Sidorenko, G.V., Gurzhiy, V.V., and Sakhonenkova, A.P., *Russ. J. Gen. Chem.*, 2022, vol. 92, no. 1, pp. 69–78.
https://doi.org/10.1134/S1070363222010108
11. Liew, H.S., Mai, C.-W., Zulkefeli, M., Madheswaran, T.,

Kiew, L.V., Delsuc, N., and Low, M.L., *Molecules*, 2020, vol. 25, no. 18, ID 4176.
https://doi.org/10.3390/molecules25184176

12. Schindler, K. and Zobi, F., *Molecules*, 2022, vol. 27, no. 2, ID 539.
https://doi.org/10.3390/molecules27020539
13. Enslin, L.E., Purkait, K., Pozza, M.D., Saubamea, B., Mesdom, P., Visser, H.G., Gasser, G., and Schutte-Smith, M., *Inorg. Chem.*, 2023, vol. 62, no. 31, pp. 12237–12251.
https://doi.org/10.1021/acs.inorgchem.3c00730
14. Guilbaud, V., Kumar, P., Grosjean, A., Delfourne, E., Boggio-Pasqua, M., Mallet-Ladeira, S., Serpentini, C.-L., Benoist, E., Dixon, I. M., and Fery-Forgues, S., *Spectrochim. Acta, Part A: Mol. Biomol. Spectrosc.*, 2026, vol. 344, ID 126647.
https://doi.org/10.1016/j.saa.2025.126647
15. Maisuls, I., Kirse, T.M., Hepp, A., Kösters, J., Wolcan, E., and Strassert, C.A., *Inorg. Chem.*, 2022, vol. 61, no. 35, pp. 13775–13791.
https://doi.org/10.1021/acs.inorgchem.2c01572
16. Miroslavov, A.E., Lumpov, A.A., Sidorenko, G.V., Levitskaya, E.M., Gorshkov, N.I., Suglobov, D.N., Alberto, R., Braband, H., Gurzhiy, V.V., Krivovichev, S.V., and Tananaev, I.G., *J. Organomet. Chem.*, 2008, vol. 693, no. 1, pp. 4–10.
https://doi.org/10.1016/j.jorganchem.2007.09.032
17. Miroslavov, A.E., Braband, H., Sidorenko, G.V., Stepanova, E.S., Lumpov, A.A., and Alberto, R., *J. Organomet. Chem.*, 2018, vol. 871, pp. 56–59.
https://doi.org/10.1016/j.jorganchem.2018.06.028
18. Miroslavov, A.E., Gurziy, V.V., Tyupina, M.Yu., Lumpov, A.A., Sidorenko, G.V., Polotskii, Yu.S., and Suglobov, D.N., *J. Organomet. Chem.*, 2013, vol. 745–746, pp. 219–225.
https://doi.org/10.1016/j.jorganchem.2013.07.019
19. Rigaku Oxford Diffraction, 2024.
20. Sheldrick, G.M., *Acta Crystallogr., Sect. A: Found. Adv.*, 2015, vol. 71, no. 1, pp. 3–8.
https://doi.org/10.1107/S2053273314026370
21. Sheldrick, G.M., *Acta Crystallogr., Sect. C: Struct. Chem.*, 2015, vol. 71, no. 1, pp. 3–8.
https://doi.org/10.1107/S2053229614024218
22. Dolomanov, O.V., Bourhis, L.J., Gildea, R.J., Howard, J.A.K., and Puschmann, H., *J. Appl. Crystallogr.*, 2009, vol. 42, no. 2, pp. 339–341.
https://doi.org/10.1107/S0021889808042726
23. Allen, F.H., Watson, D.G., Brammer, L., Orpen, A.G., and Taylor, R., in *International Tables for Crystallography*, Prince, E., Ed., Chester, England: International Union of *Crystallography,* 2006, 1st ed., vol. C, pp. 790–811.
https://doi.org/10.1107/97809553602060000621
24. Kinzhalov, M.A., Kashina, M.V., Mikherdov, A.S., Mozheeva, E.A., Novikov, A.S., Smirnov, A.S., Ivanov, D.M., Kryukova, M.A., Ivanov, A.Yu., Smirnov, S.N., Kukushkin, V.Yu., and Luzyanin, K.V., *Angew. Chem. Int. Ed.*, 2018, vol. 57, no. 39, pp. 12785–12789.
https://doi.org/10.1002/anie.201807642
25. Zakrzewski, J., Huras, B., and Kiełczewska, A., *Synthesis*, 2015, vol. 48, no. 01, pp. 85–96.
https://doi.org/10.1055/s-0035-1560481
26. Sidorenko, G.V., Miroslavov, A.E., Tyupina, M.Yu., Gurzhiy, V.V., Sakhonenkova, A.P., and Lumpov, A.A., *Inorg. Chem.*, 2023, vol. 62, no. 38, pp. 15593–15604.
https://doi.org/10.1021/acs.inorgchem.3c02204
27. Neese, F., *WIREs Comput. Mol. Sci.*, 2025, vol. 15, no. 2, ID e70019.
https://doi.org/10.1002/wcms.70019
28. Tao, J., Perdew, J.P., Staroverov, V.N., and Scuseria, G.E., *Phys. Rev. Lett.*, 2003, vol. 91, no. 14, ID 146401.
https://doi.org/10.1103/PhysRevLett.91.146401
29. Sanad, M.H. and Borai, E.H., *Radiochim. Acta*, 2015, vol. 103, no. 12, pp. 879–891.
https://doi.org/10.1515/ract-2015-2428
30. Grimme, S., Antony, J., Ehrlich, S., and Krieg, H., *J. Chem. Phys.*, 2010, vol. 132, no. 15, p. 154104.
https://doi.org/10.1063/1.3382344
31. Canal Neto, A., Ferreira, I.B., Jorge, F.E., and De Oliveira, A.Z., *Chem. Phys. Lett.*, 2021, vol. 771, ID 138548.
https://doi.org/10.1016/j.cplett.2021.138548
32. Pritchard, B.P., Altarawy, D., Didier, B., Gibson, T.D., and Windus, T.L., *J. Chem. Inf. Model.*, 2019, vol. 59, no. 11, pp. 4814–4820.
https://doi.org/10.1021/acs.jcim.9b00725
33. Ren, X., Rinke, P., Blum, V., Wieferink, J., Tkatchenko, A., Sanfilippo, A., Reuter, K., and Scheffler, M., *New J. Phys.*, 2012, vol. 14, no. 5, ID 053020.
https://doi.org/10.1088/1367-2630/14/5/053020
34. Stoychev, G.L., Auer, A.A., and Neese, F., *J. Chem. Theory Comput.*, 2017, vol. 13, no. 2, pp. 554–562.
https://doi.org/10.1021/acs.jctc.6b01041
35. Van Lenthe, E., Baerends, E.J., and Snijders, J.G., *J. Chem. Phys.*, 1994, vol. 101, no. 11, pp. 9783–9792.
https://doi.org/10.1063/1.467943

36. Van Lenthe, E., Snijders, J.G., and Baerends, E.J., *J. Chem. Phys.*, 1996, vol. 105, no. 15, pp. 6505–6516. https://doi.org/10.1063/1.472460
37. Van Lenthe, E., Ehlers, A., and Baerends, E.-J., *J. Chem. Phys.*, 1999, vol. 110, no. 18, pp. 8943–8953. https://doi.org/10.1063/1.478813
38. Van Lenthe, E., Van Leeuwen, R., Baerends, E.J., and Snijders, J.G., *Int. J. Quantum Chem.*, 1996, vol. 57, no. 3, pp. 281–293. https://doi.org/10.1002/(SICI)1097-461X(1996)57:3%3C281::AID-QUA2%3E3.0.CO;2-U
39. Barone, V. and Cossi, M., *J. Phys. Chem. A*, 1998, vol. 102, no. 11, pp. 1995–2001. https://doi.org/10.1021/jp9716997
40. Bader, R.F.W., *Chem. Rev.*, 1991, vol. 91, no. 5, pp. 893–928. https://doi.org/10.1021/cr00005a013
41. Lu, T., *J. Chem. Phys.*, 2024, vol. 161, no. 8, p. 082503. https://doi.org/10.1063/5.0216272
42. https://www. chemcraftprog.com
43. Miroslavov, A.E., Kuz'min, V.V., Sakhonenkova, A.P., Tyupina, M.Yu., Sidorenko, G.V., Kochergina, A.R., and Polukeev, V.A., *Radiochemistry*, 2023, vol. 65, no. 6, pp. 672–679. https://doi.org/10.1134/S1066362223060085
44. Miroslavov, A.E., Kuz'menko, P.M., Tyupina, M.Yu., Sakhonenkova, A.P., Sidorenko, G.V., Kochergina, A.R., and Krotov, S.A., *Radiochemistry*, 2024, vol. 66, no. 4, pp. 522–530. https://doi.org/10.1134/S1066362224040143
45. Tsubaki, H., Tohyama, S., Koike, K., Saitoh, H., and Ishitani, O., *Dalton Trans.*, 2005, no. 2, pp. 385–395. https://doi.org/10.1039/B407947G
46. Claude, G., Salsi, F., Hagenbach, A., Gembicky, M., Neville, M., Chan, C., Figueroa, J.S., and Abram, U., *Organometallics*, 2020, vol. 39, no. 12, pp. 2287–2294. https://doi.org/10.1021/acs.organomet.0c00238
47. Claude, G., Puccio, D., Roca Jungfer, M., Hagenbach, A., Spreckelmeyer, S., and Abram, U., *Inorg. Chem.*, 2023, vol. 62, no. 31, pp. 12445–12452. https://doi.org/10.1021/acs.inorgchem.3c01638
48. O'Connell, L.A., Dewan, J., Jones, A.G., and Davison, A., *Inorg. Chem.*, 1990, vol. 29, no. 18, pp. 3539–3547. https://doi.org/10.1021/ic00343a049
49. Csonka, I.P., Szepes, L., and Modelli, A., *J. Mass Spectrom.*, 2004, vol. 39, no. 12, pp. 1456–1466. https://doi.org/10.1002/jms.761
50. Miroslavov, A.E., Polotskii, Y.S., Gurzhiy, V.V., Ivanov, A.Yu., Lumpov, A.A., Tyupina, M.Yu., Sidorenko, G.V., Tolstoy, P.M., Maltsev, D.A., and Suglobov, D.N., *Inorg. Chem.*, 2014, vol. 53, no. 15, pp. 7861–7869. https://doi.org/10.1021/ic500327s
51. Hasegawa, S., Masuda, S., Takano, S., Harano, K., and Tsukuda, T., *ACS Catal.*, 2022, vol. 12, no. 11, pp. 6550–6558. https://doi.org/10.1021/acscatal.2c01355
52. Allerhand, A. and Von Rague Schleyer, P., *J. Am. Chem. Soc.*, 1963, vol. 85, no. 7, pp. 866–870. https://doi.org/10.1021/ja00890a006
53. Kanzow, A., Suhm, M.A., and Bödecker, M., *ChemPhysChem*, 2026, vol. 27, no. 5, ID e202500834. https://doi.org/10.1002/cphc.202500834
54. Miroslavov, A.E., Babitova, E.S., Brechalov, A.A., Gurzhiy, V.V., Sakhonenkova, A.P., Ivanov, D.M., Tyupina, M.Yu., Gavrishchuk, S.O., and Tupikina, E.Yu., *Inorg. Chem.*, 2026, vol. 65, no. 26, pp. 15200–15211. https://doi.org/10.1021/acs.inorgchem.6c02170
55. Kuznetsov, V.V., Poineau, F., German, K.E., and Filatova, E.A., *Commun. Chem*, 2024, vol. 7, no. 1, p. 259. https://doi.org/10.1038/s42004-024-01349-2
56. Miroslavov, A.E., Kochergina, A.R., Sidorenko, G.V., Gurzhiy, V.V., Sakhonenkova, A.P., Gusev, E.G., Chisty, L., and Tyupina, M.Yu., *Inorg. Chem.*, 2025, vol. 64, no. 31, pp. 16073–16087. https://doi.org/10.1021/acs.inorgchem.5c02391
57. Chakraborty, I., Jimenez, J., Sameera, W.M.C., Kato, M., and Mascharak, P. K., *Inorg. Chem.*, 2017, vol. 56, no. 5, pp. 2863–2873. https://doi.org/10.1021/acs.inorgchem.6b02999

Publisher's Note. Pleiades Publishing remains neutral with regard to jurisdictional claims in published maps and institutional affiliations.
AI tools may have been used in the translation or editing of this article.